DMI
Ministry of Climate and Energy

Scientific Report 12-04

Hydrometeor Classification using Polarimetric C-band Dopplar Weather Radars

Rashpal S. Gill, Martin B. Sørensen and Thomas Bøvith

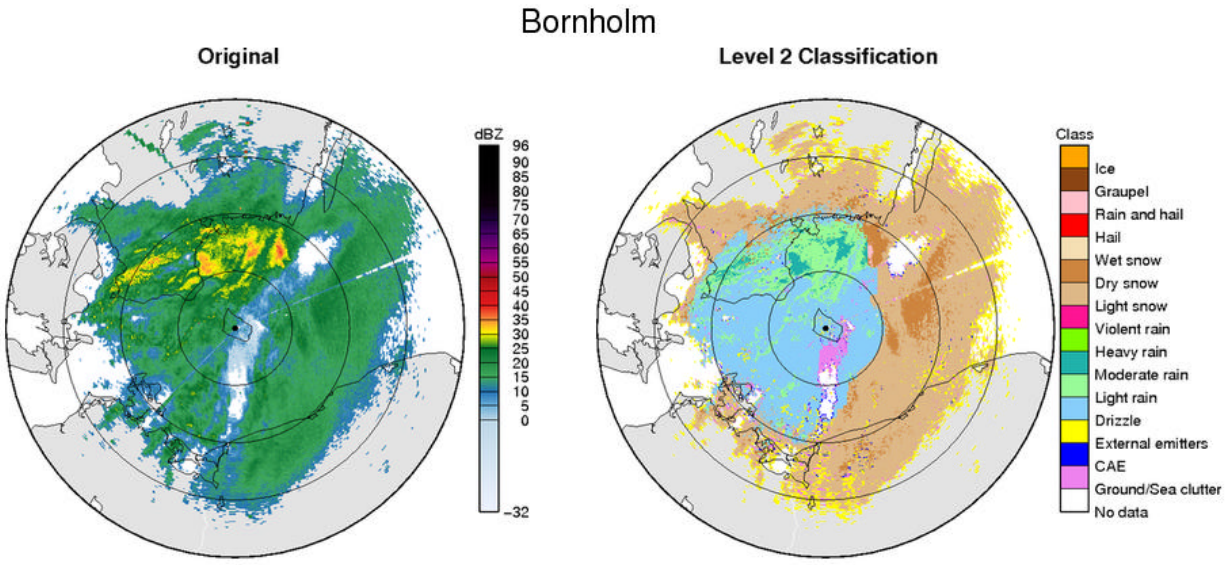

Copenhagen 2012

Colophon

Serial title:
Scientific Report 12-04

Title:
Hydrometeor Classification using Polarimetric C-band Dopplar Weather Radars

Subtitle:

Author(s):
Rashpal S. Gill, Martin B. Sørensen and Thomas Bøvith

Other contributors:

Responsible institution:
Danish Meteorological Institute

Language:
English

Keywords:
Dual polarization weather radars. Rain path attenuation correction. Fuzzy logics. Hydrometeors.

Url:
www.dmi.dk/dmi/sr12-04

Digital ISBN:
978-87-7478-614-6

ISSN:
1399-1949

Version:
15th October 2012

Website:
www.dmi.dk

Content:

Abstract 4
Resumé 4
1. Introduction 5
2. Radar data quality 7
3. Melting layer determination 11
4. Estimation of specific differential phase 12
4.1 Computation procedure 12
5. Rain attenuation correction 13
5.1 Radar reflectivity rain attenuation correction 15
5.2 Radar differential reflectivity rain attenuation correction 16
5.3 Computation procedure 16
6. Hydrometeor classifier 18
6.1 Introduction 18
6.2 Hydrometeor classes 18
6.3 Membership functions 18
6.4 Output from the hydrometeor classifier 20
6.5 Computational procedure 23
7. Summary 25
Acknowledgements 26
References 27
Previous reports 29

Abstract

A hydrometeor classifier (HMC) using dual polarization C-band Dopplar weather radar observations has been developed with partial funding from the EU financed project BALTRAD (Baltic Sea Region Programme 2007-2013).

Prior to the development of the HMC a number of investigations were undertaken to determine the sensitivity of the dual polarization parameters to, amongst others, the orange peel radomes used at the Danish Meteorological Institute (DMI). A number of data quality software tools to monitor the temporal variability of the parameters are now in operation, including a dedicated radar scan at 90 deg. elevation.

The classification scheme is based on fuzzy logic and the membership functions are represented by 1 dimensional Beta functions.

In the current version, the algorithm can undertake the so-called level 1 and level 2 classifications. In the level 1 classification a radar echo is classified into one of four simple classes: precipitation, clutter, clean air echoes, and electrical signals from external emitters. Similarly, in the case of level 2 classification a radar echo is classified into one of 12 classes; ground clutter, sea clutter, external emitters, clean air echoes, drizzle, light rain, moderate rain, heavy rain, violent rain, light snow, moderate to heavy snow and hail/rain mixture. In the level 2 classification the melting layer heights from the numerical weather prediction model are used to aid the classification. Melting layer determination algorithm using the dualpol parameters alone has also been developed as part of the HMC. This algorithm is under going evaluations before its use in the HMC scheme.

One of the by product of the HMC algorithm as been that it can be used to remove the non-meteorological echoes in, amongst others, the original radar reflectivity product, Z_{HH}. This product has been much appreciated by the DMI's end users, such as the operational meteorologists, and, not surprisingly, it was the first 'HMC' product to be put into operational use.

In the future, further improvements to the algorithm are planned such as fine tuning the membership functions for hail. As hail is observed in very small regions occupying few pixels, it has been a challenge to extract these cells in the radar data whilst ensuring they are not contaminated by other hydrometeor classes.

The algorithm has now been incorporated into the BALTRAD repository, the so-called toolbox. EU funding rules require the software to be made available according to open source principles. This means the software, including the computer source code, is now available to the project partners and third parties including commercial entities. The copy rights still reside with DMI.

Resumé

1. Introduction

DMI operates five weather radars, two of which, at Virring in central Jutland (56.024 °N, 10.025 °E) and on the island of Bornholm (55.113 °N, 14.999 °E) have dual polarization capabilities. These radars measure in addition to the four parameters measured by the traditional Doppler radars; uncorrected reflectivity (U), corrected reflectivity (Z_{HH}), radial doppler velocity (V), spectral width (W), also the differential reflectivity (Z_{DR}), differential phase shift (Φ_{DP}), specific differential phase (K_{DP}), co-polar correlation coefficient (r_{HV}) and linear depolarization ratio (LDR). These latter five so-called dual polarization parameters ($Z_{DR,}$ $\Phi_{DP,}$ $K_{DP,}$ r_{HV}, LDR) are sensitive to the properties of the returned echo such as its shape, size and orientation, its physical state and hydrometeor class (Bringi and Chandrasekar, 2001). In particular, Z_{DR} is sensitive to the shape of the hydrometeors and typically have values ~0.0 dB for small rain drops of size <0.3 mm and increases in value for larger drop size as can be seen in figure 1. It thus has the potential to discriminate between light and heavy precipitation and for detecting hail. Similarly, r_{HV}, is useful for discriminating between precipitation and non-meteorological echoes. It is also sensitive to the physical state of the hydrometeors such as solid/liquid phase and is thus useful for detecting the melting layer. K_{DP} is sensitive to isotropic/anisotropic precipitation regions and is important for estimating rain rates and for rain attenuation corrections for Z_{HH} and Z_{DR}. Finally, LDR is also sensitive to the shape and orientation and dielectric constant of the precipitation particles so that wet non spherical particles results in large LDR whilst drizzle and dry ice particles are associated with low LDR (Bringi and Chandrasekar, 2001).

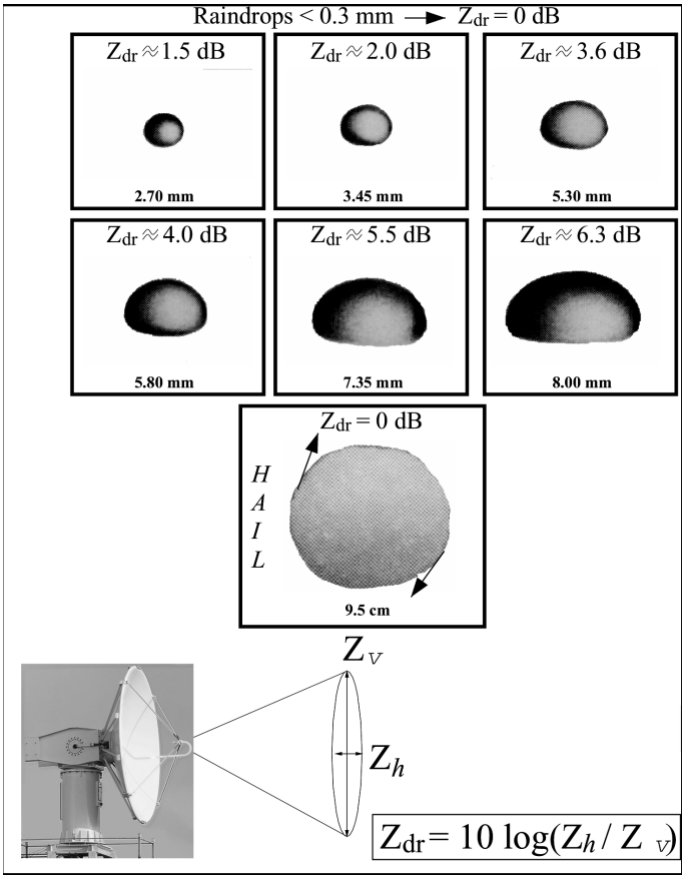

Fig. 1 Summary of typical Z_{DR} values of raindrops of various sizes and hail (Bringi and Chandrasekar, 2001).

From above it is clear that all the dual polarization parameters contain some information that is useful for radar echo discrimination. In most of the cases the range of values of the radar parameters, for the different hydrometeor classes, are overlapping. Thus how to combine the information in these parameters into useful operational products has been a challenge. A number of methods using neural networks, Boolan decision trees, statistical methods using probabilities and fuzzy logic have been tried (Bringi and Chandrasekar, 2001). However, in the last 10 – 15 years the method based on the fuzzy logic technique has become the preferred choice as it is well suited for combining the information from the overlapping hydrometeor classes from the different radar parameters. There are several articles in the literature describing various aspects of fuzzy logic hydrometeor classification (Bringi and Chandrasekar, 2001, Zrnic et. al., 2001, Schuur et. al., 2003, Lim et. al., 2005).

Finally, DMI acquired its two dual polarization weather radars on Bornholm and Virring in 2007 and 2009, respectively. The results presented in this report have been under development since 2008 (Gill et al., 2008, 2010 and 2012).

2. Radar data quality

As stated above fuzzy logic techniques are used for hydrometeor classification because they can deal with the overlapping classes from the different radar parameters. However, for reliable hydrometeor classification it is very important to have good quality radar observations. In particular, previous studies have concluded that Z_{DR} has to be accurate to within 0.1 – 0.2 dB, $\Phi_{DP}(0)$ within 1° or better, r_{HV} greater than 0.98 in light to moderate rain (Sugier et. al., 2006). If these conditions are not met then all the products, including those from the HMC, derived using the dual polarization parameters will be affected by noise so that the distinction between rain and wet snow, for example, will be difficult. Apart from requiring radar observation to be of very high quality, previous studies have also shown that, unlike the radar parameters from the traditional Doppler radars, the dual polarization radar parameters from the C-band radars that DMI operates are very sensitive to the radar hardware such as the radome, thermal noise in the receiver etc. (Sugier et. al., 2006). To ascertain the sensitivity of the dual polarization parameters to these radar hardware issues a number of investigations were undertaken at DMI. As a way of example, fig. 2 shows the sensitivity of the differential reflectivity parameter to the radome at Bornholm. Our investigations have shown that the maximum of Z_{DR} values are directly correlated with the positions of the bolts used to join the eight panels of the orange peel radome. Also note that Z_{DR} varies by as much as ± 0.2 dB which is, given what is stated above, barely tolerable. However, knowing the sensitivity of Z_{DR} to the physical properties of the radar radomes at Bornholm and Virring is important so that techniques can be developed to mitigate this effect (see later).

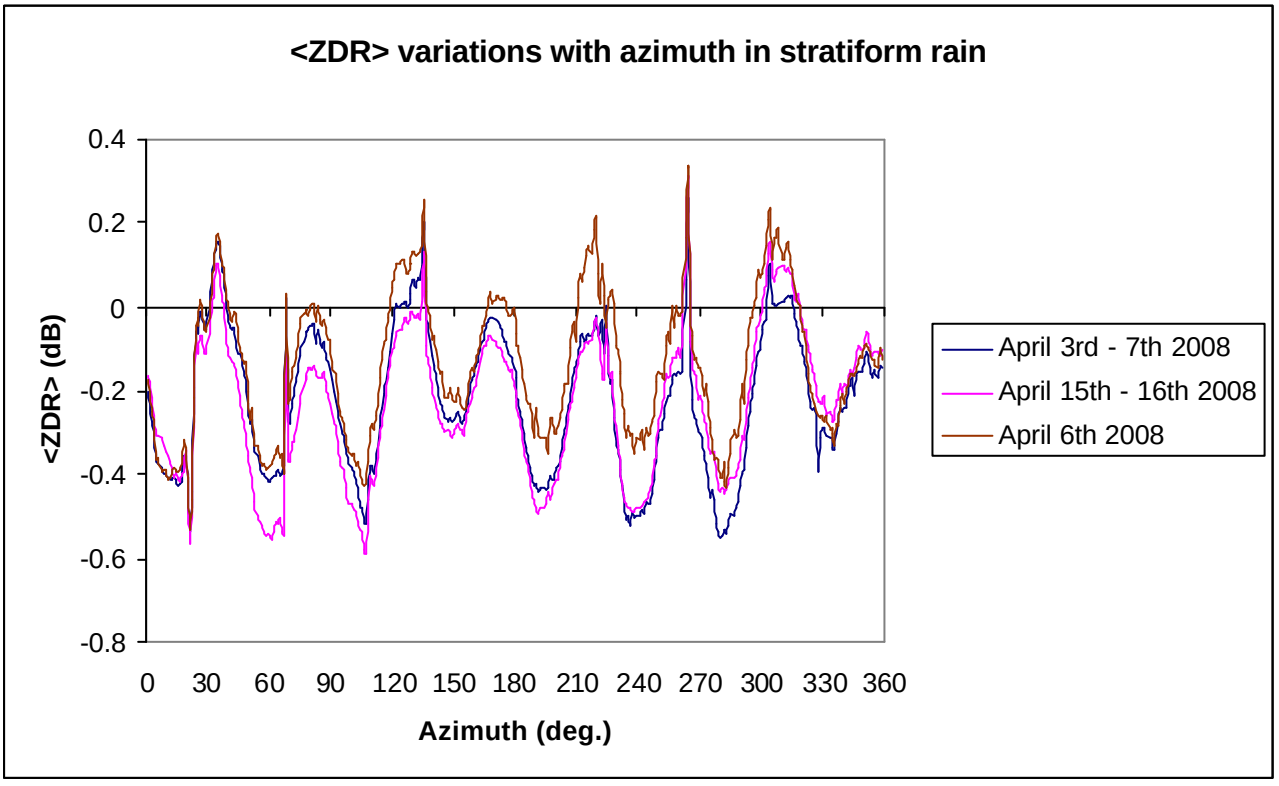

Fig. 2 Shows the variation of the Z_{DR} parameter to the radome at the Bornholm radar.

In addition to analysing the effects of radar radomes on the dual polarization parameters, a number of other monitoring indicators have been developed which measure the quality of the radar parameters. In particular, the monitoring indicators that were computed are the following (Sugier et. al.,

2006, Boumahmoud et. al, 2010):

(i) Z_{DR} in light rain between 20 dBZ – 22 dBZ at close range (requirement: Z_{DR} has to be accurate to within 0.1 – 0.2 dB)

(ii) $\Phi_{DP}(0)$ offsets using the first 5 consecutive gates containing precipitation (requirement: variations of $\Phi_{DP}(0)$ within 1° or better)

(iii) upper 75% quantile r_{HV} in rain (requirement: r_{HV} greater than 0.98 in light to moderate rain)

(iv) special radar scans at 90° elevation is performed to estimate the potential biases in Z_{DR} (expected to be near 0.0 dB for a well calibrated radar).

The above parameters are computed daily to ascertain their temporal variability so that realistic temporal corrections can be applied to the data. As a way of example, figure 3 shows, the diurnal variations of Z_{DR} in light rain, $\Phi_{DP}(0)$ offsets and r_{HV} in rain, from both the radars at Bornholm and Virring, respectively.

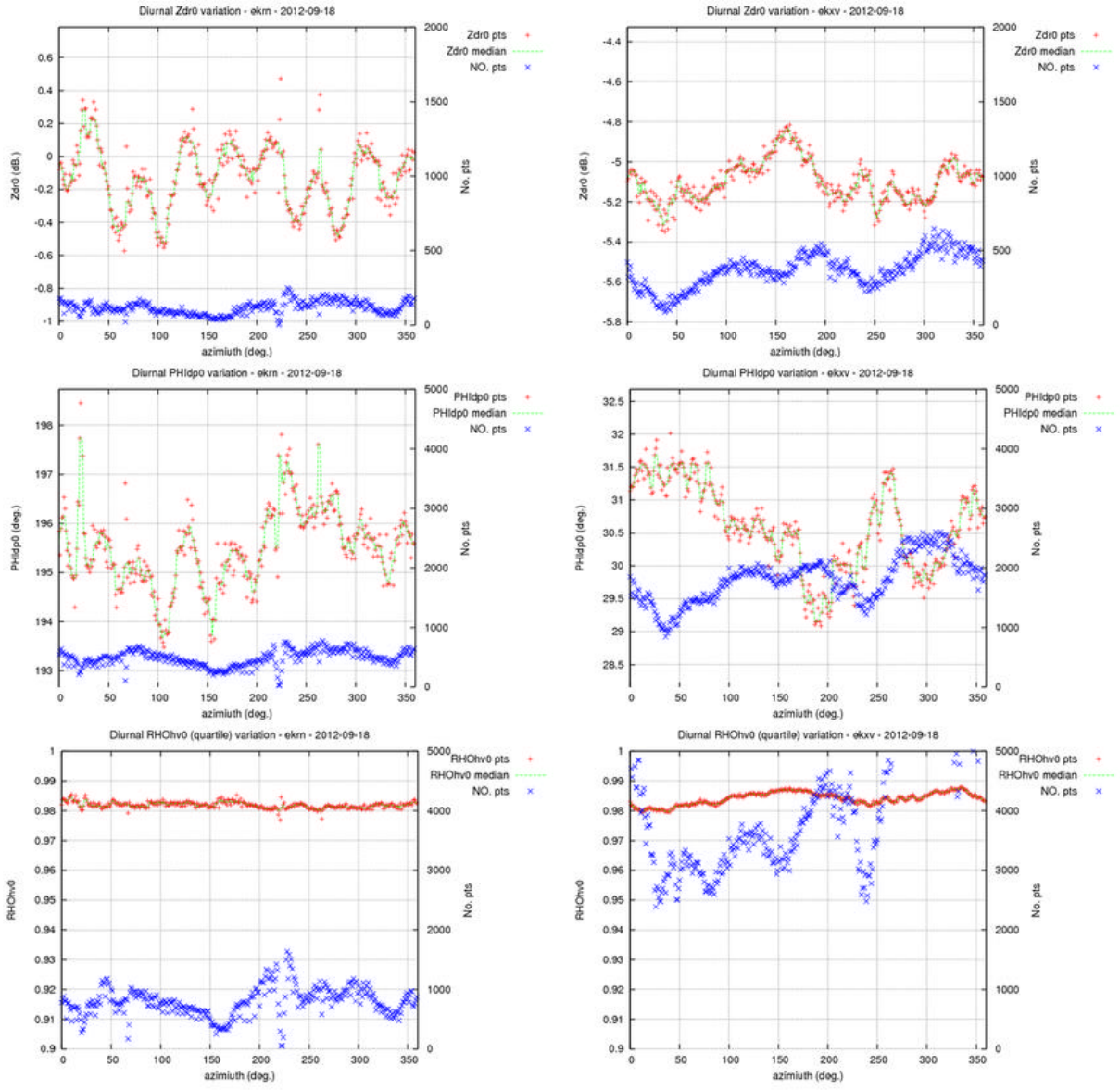

Fig. 3 The diurnal variations of Z_{DR}, $\Phi_{DP}(0)$ and r_{HV} *(colour red) as a function of azimuth in rain from18th September 2012 for Bornholm (left column) and Virring (right column) radars. The*

curves in blue are the corresponding number of r_{HV} points that fulfilled the diagnostic criteria.

It can be seen from fig. 3 that both Z_{DR} and $\Phi_{DP}(0)$ are clearly affected by the radome at the Bornholm, whilst the radome effects in these parameters from the Virring radar are not as clearly discernable. The main reason of the latter is that whilst the radome at Bornholm consists of 8 panels, the one at Virring consists of 12 such panels, which result in overlapping effects from the individual panels. Nevertheless, it can be clearly seen that the radome "noise" in both Z_{DR} and $\Phi_{DP}(0)$ is significantly less in the Virring radar than in the Bornholm radar. Attempts have been made to remove the effects of the radomes on these two dual polarization parameters. The results can be seen in fig. 4. It can be seen from this figure that we have been able to remove the obvious sinusoidal variations in both Z_{DR} and $\Phi_{DP}(0)$. However, the techniques used need further improvement. Thus the conclusion so far is that both Z_{DR} and Φ_{DP} do not 100% meet the data quality requirements outlined above i.e., Z_{DR} has to be accurate to within 0.1 – 0.2 dB and Φ_{DP} has to be accurate to within 0.1 – 0.2 dB.

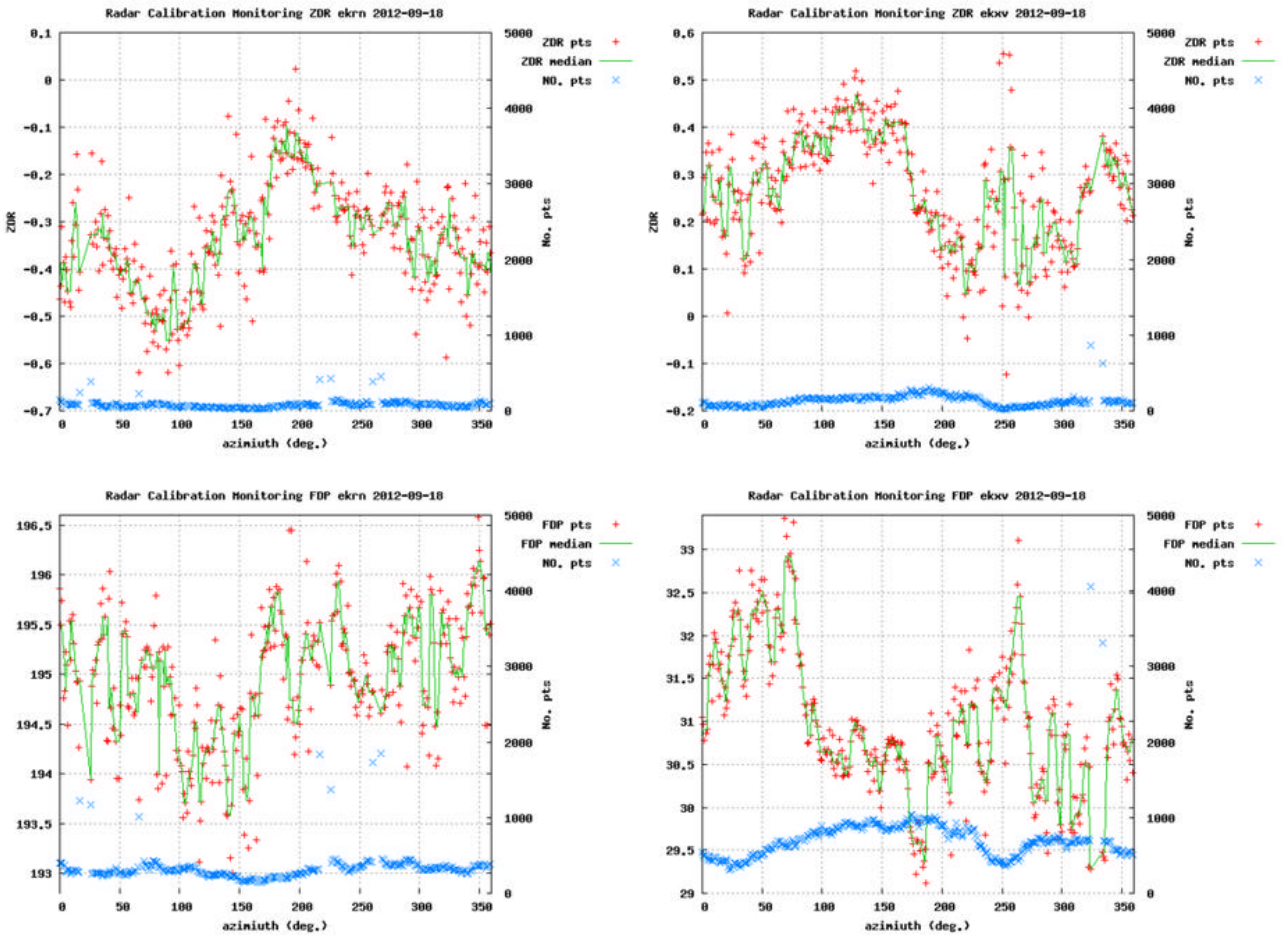

Fig. 4 The corrected diurnal variations of Z_{DR} and Φ_{DP} (colour red) as a function of azimuth in rain from18th September 2012 for Bornholm and Virring radars, left and right columns respectively. The curves in blue are the corresponding number of r_{HV} points that fulfilled the diagnostic criteria.

However, contrary to Z_{DR} and Φ_{DP}, it can be seen from fig. 3 the variation of r_{HV} from the two radars meets the quality requirements i.e., r_{HV} greater than 0.98 in light to moderate rain.

Similarly, fig. 5 shows the results from the special radar scans at 90º elevation to estimate the potential biases in Z_{DR} (expected to be near 0.0 dB).

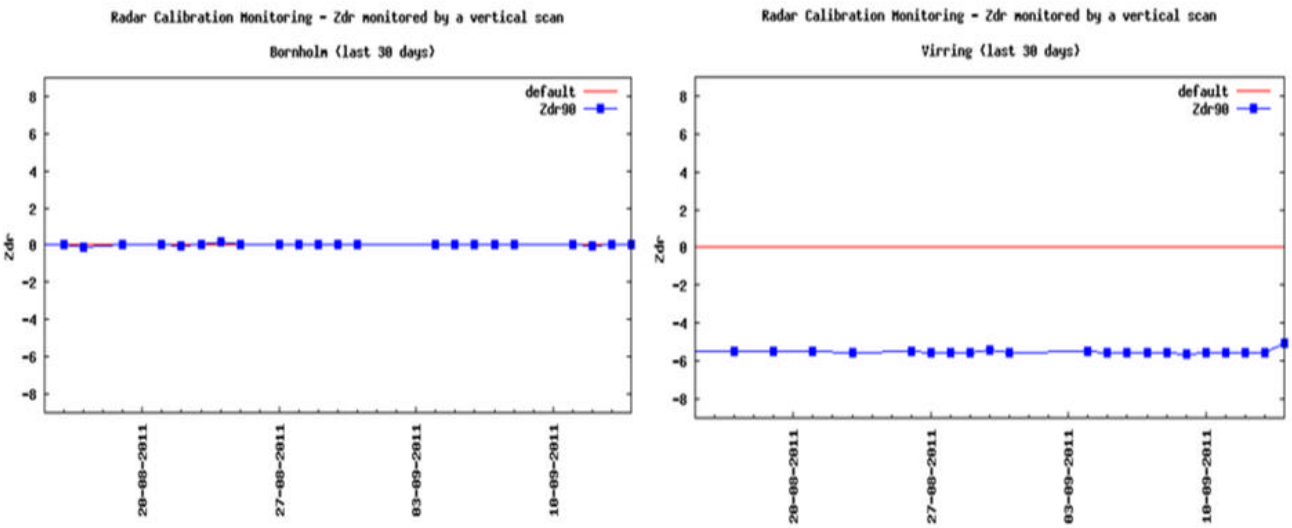

Fig.5 The diurnal biases in the Z_{DR} parameter for the Bornholm and Virring radars, computed using the radar scan at 90º elevation.

From theoretical considerations, the values of Z_{DR} in rain for the 90º elevation scan should be ~ 0.0 dB (Sugier et. al., 2006). However, from the figures it can be seen that whilst Z_{DR} parameter of the Bornholm radar meets this quality requirement, this is not the case for the radar at Virring. The latter shows biases of ~ - 5.5 dB which is very large given that Z_{DR} should generally lie in the range ~ 0 dB - 6.0 dB in precipitation. Nevertheless, knowing these biases is very important so that corrective techniques can be developed and implemented.

3. Melting layer determination

One of the key parameters in developing the hydrometeor classifier is determining the height of melting layer (ML). For the latter, a melting layer determination algorithm has been developed based on the previous studies in the open literature using the dual polarization moments Z_{DR}, Z_{HH} and r_{HV} (Giangrande et. al., 2008). It has been found that this algorithm gives very favourable results when compared to the Numerical Weather Prediction (NWP) model at short lead times (1 – 2 hours). Unfortunately, a ML algorithm based solely on the dual polarization parameters, requires sufficiently full radar volumes and the use of higher elevation scans for reliable results. These conditions are difficult to meet in routine operations. To overcome this problem it has been necessary to supplement the ML heights determined using the radar data alone with those estimated using the wet bulb temperature profiles from the NWP model forecast. Fig. 6 shows an example of the output from the ML algorithm. In particular, the figure shows the top and the bottom of the melting levels computed from radar ML algorithm superimposed on the height of the 0 ºC wet bulb temperature from NWP model forecast. As can be seen from the figure the agreement between the two is surprisingly good, given that what the radar actually measure is not the temperature of the hydrometeors but rather the change in their physical state, as measured by the radar's dual polarization parameters, as they fall past the 0 ºC isotherm.

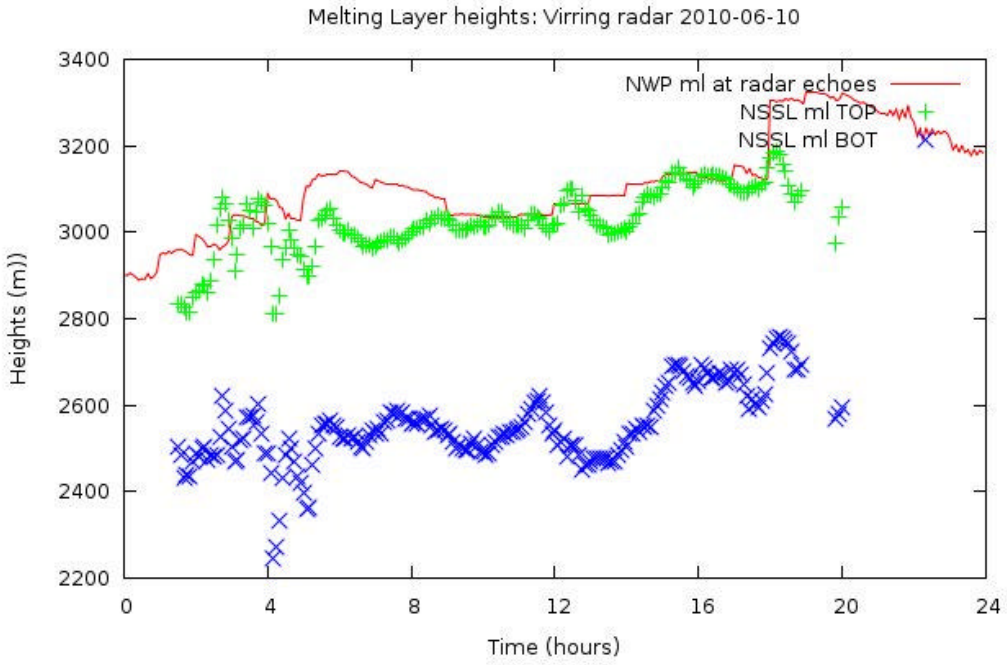

Fig. 6 Shows the top (green) and bottom (blue) of the melting layer computed using the radar algorithm superimposed on the one computed by the local NWP forecast model(red).

4. Estimation of specific differential phase

The specific differential phase, K_{DP} (deg./km), is an important parameter for rain rates estimates and is also sensitive to the shape of hydrometeors. In particular, it is positive for horizontally oriented oblate particles and negative for vertically oriented prolates (Bringi and Chandrasekar, 2001). Furthermore, it has a number of advantages compared to the traditional reflectivity, Z_{HH}. For example, it is independent of transmitter and receiver calibration, unaffected by rain attenuation and not affected by rain on radome (Bringi et. al., 2005).

Unfortunately, K_{DP} is not available from the radar processing software provided by the radar manufacturer. It has to be thus estimated. It is related to the derivative of the differential phase, $\Phi_{DP}(r)$ along the radar range by the following expression

$$K_{DP}(r) = \frac{1}{2} \cdot \frac{d}{dr} \Phi_{DP}(r) \tag{1}$$

4.1 Computation procedure

Computing K_{DP} is rather challenging as the underlying $\Phi_{DP}(r)$ values are very "noisy" i.e., generally contain many outliers. The current method used at DMI was inspired by Bringi et al. (2005) and involve the following steps:

1. Compute the texture of Φ_{DP}, Tex($\Phi_{DP(x,y)}$), using the following expression:

$$Tex(\Phi_{DP(x,y)}) = \sqrt{\frac{\sum_{i=-(R-1)/2}^{(R-1)/2} \sum_{j=-(A-1)/2}^{(A-1)/2} (\Phi_{DP(x,y)} - \Phi_{DP(x+i,y+j)})^2}{R \cdot A}} \tag{2}$$

   where R and A are the sizes of the computation windows in the range and azimuth directions. In the current version, for the estimation of Tex($\Phi_{DP(x,y)}$), both R and A have been set to 3 gates each of size 500m.

2. Generate range mask based on thresholds for Tex($\Phi_{DP(x,y)threshold}$), Signal-to-Noise Ratio ($SNR_{threshold}$) and $r_{HVthreshold}$ to remove bad Φ_{DP} values.

3. Interpolate Φ_{DP} across "bad" data segments.

4. $\Phi_{DP}(r)$ is then smoothed using a median filter with a window size of ~ 5.0 km -6.5 km.

5. K_{DP} is then estimated by fitting a straight line (linear regression) on the above window.

5. Rain attenuation correction

As electromagnetic waves propagate through precipitation filled medium, they suffer both absorption and scattering. These quantities are dependant on the wavelength of the incident waves, diameter of the drops and on the temperature. Further, when the rain drops are non-spherical then these parameters also depend on the polarization of the incident waves (Doviak and Zrnic, 1993).

In the case of when the ration of drop, D, to wavelength, l , is small, then for spherical drops the following approximation for the absorption and scattering coefficients, s_a and s_s are obtained (Doviak and Zrnic, 1993)

$$s_a \approx (p^2 D^3 / l) \mathrm{Im}(-K_m) \tag{3}$$

$$s_s \approx (2p^5 D^6 / 3l^4) |K_m|^2 \tag{4}$$

where $K_m=(m^2-1)/(m^2+2)$ and m=n-jk is complex refractive index for water. The refractive index in n and k is the attenuation index and is function of both wavelength and temperature. Im refers to the imaginary part of K_m.

The sum of s_a and s_s is defined as the attenuation or extinction cross section, s_{ext} .

The attenuation coefficient or the specific attenuation, for a horizontally or vertically polarized waves, (A_h or A_v) respectively, in dB/km is given by the following expression

$$A_{h,v} = 4.343 \cdot 10^3 \int s_{ext}^{h,v} N(D) dD \tag{5}$$

Thus knowing the drop size distribution, N(D), and the extinction coefficient it is possible to estimate the amount of attenuation electromagnetic waves suffer as they transverse through rain infested medium. There are no easy solutions to the above equation (Doviak and Zrnic, 1993). Traditionally one has tried to solve it numerically by assuming power laws for the extinction coefficient and a distribution for the drop size distribution. This resulted in a one way attenuation coefficient valid at particular temperature and wavelength (Doviak and Zrnic, 1993). For example, at 5 cm and temperature of ~ 18 ºC, the one-way specific attenuation is given by the well known power law of the type

$$A_r = K \cdot R^b \tag{6}$$

where K and b are constants typically ~ 0.0018 and 1.05, respectively, and R is the rain rate in mm/h and A_r in dB/km.

Instead of relating specific attenuation coefficient to the rain rates as in equation (6) above, in the case of dual polarization parameters, however, the specific attenuation coefficients A_h or A_v are generally expressed as a function of the differential phase, Φ_{DP}, as these relations are recognised to

be more accurate (Bring and Chandrasekar, 2001). The complete theoretical background to this subject is beyond the scope of this report; the interested reader is referred to Bring and Chandrasekar, 2001.

However, a summary of the most pertinent relations are repeated below.

At frequencies > 3 GHz but < 15 GHz a good approximation to the extinction cross section, s_{ext}, up to the order $(D/l)^5$ can be obtained. The resulting expression for s_{ext} as a function of rain drop diameter is illustrated in figure 7.

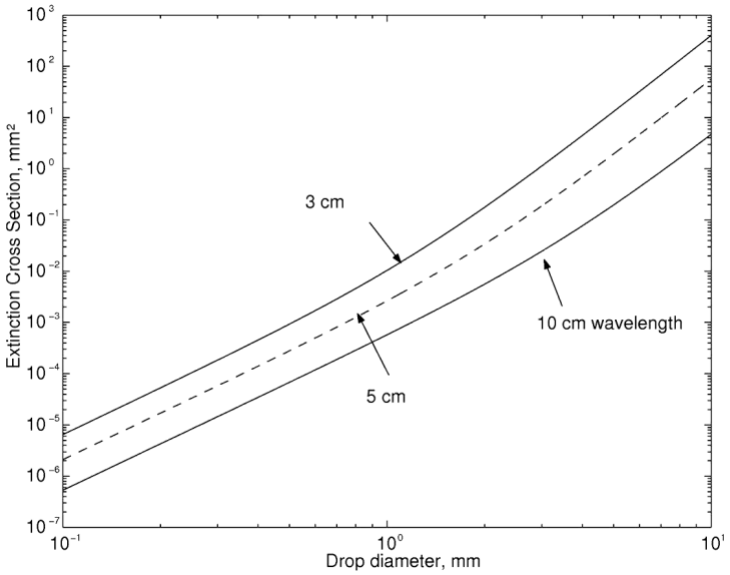

Fig. 7 Extinction cross section of spherical drops versus drop diameter (Bringi and Chanderasekar, 2001, p. 491).

From fig. 7 it is clear that a power-law relationship of the type $s_{ext} = C_l \cdot D^n$ is feasible where C_l is wavelength dependant constant and D is drop diameter. At C-band when drop sizes are in the range $0 \cdot 1 \le D \le 8mm$ n ~ 3.9, while $5 \le D \le 10mm$ n ~ 4.8, respectively. Assuming n ~ 4 for simplicity in the above expression for s_{ext} and substituting it into equation (5) above results in the following expression for the specific attenuation

$$A_{h,v} = 4.343 \cdot 10^3 \cdot C_l \int D^4 N(D) dD \qquad (7)$$

In order to relate the above specific attenuation coefficient to the differential propagation phase, it is noted that the specific differential phase, K_{DP} (deg./km), is given by the following expression

$$K_{DP} \approx \left(\frac{180}{l}\right) 10^{-3} CW(0.062 D_m) \quad (8)$$

Where C is constant, typically ~ 3.75, W is the total rainwater content (in units of g m^{-3}), D_m is the mass weighted mean diameter (units of mm) and l in units of m. It is noted that

$$W \cdot D_m \propto \int D^4 N(D) dD \quad (9)$$

(Bringi and Chanderasekar).

It follows from equations (7) – (9) that in the case of the horizontally polarized waves, the specific attenuation coefficient can be expressed as

$$A_h = a \cdot K_{DP}^b \quad (10)$$

where a and b are constants which typically have values ≈ 0.08 dB/deg. and 1, respectively, at C-band.

Using the above expression for A_h it is possible to estimate the amount attenuation suffered by the weather radar reflectivity parameter, Z_{HH}.

A number of methods have been proposed in the literature for correcting Z_{HH} for rain attenuation (Bringi el. al., 1990, Carey et al., 2000, Tesud et. al., 2000, Bringi et al., 2001). Describing each one of these is beyond the scope of this report. However, it is suffice to state that from an operational point of view, the so-called "Linear Φ_{DP} with a fixed linear a", by Bringi et. al., (1990) is preferred as it is easy to implement in real-time and is not too demanding computationally. However, its main dis-advantage is that it can over or under-estimate attenuation. In the current version of the software, this method has been implemented to correct for the attenuation suffered by Z_{HH} and Z_{DR} in rain and is described next.

5.1 Radar reflectivity rain attenuation correction

For an inhomogeneous path, i.e., A_h varies along the path, the corrected Z_{HH} (units of dB) is related to the measured $Z_{HH}^{measured}$ at range r from the radar by the following expression

$$Z_{HH}(r) = Z_{HH}^{measured}(r) + 2\int_0^r A_h(r) dr \quad (11)$$

Substituting equation (10) into the above expression and assuming a is constant we get

$$Z_{HH}(r) = Z_{HH}^{measured}(r) + 2a\int_0^r K_{DP}(r) dr \quad (12)$$

Now substituting for K_{DP} from equation (1), the following expression is obtained for the corrected Z_{HH}

$$Z_{HH}^{corrected}(r) = Z_{HH}^{measured}(r) + a\left[\Phi_{DP}(r) - \Phi_{DP}(0)\right] \quad (13)$$

Thus knowing by how much Φ_{DP} increases from its value at the origin $\Phi_{DP}(0)$ it is possible to correct the radar reflectivity, Z_{HH}

5.2 Radar differential reflectivity rain attenuation correction

Just like the above radar horizontal reflectivity, Z_{HH} , the differential reflectivity also suffer from rain attenuation, especially at C- and X-bands. To estimate the rain attenuation of Z_{DR}, we repeat the above procedure for Z_{HH}. We get in this case the following expression

$$Z_{DR}^{corrected}(r) = Z_{DR}^{measured}(r) + 2\int_0^r A_{DP}(r)dr \quad (14)$$

where A_{DP} is the difference between the specific attenuations between the horizontally and vertically polarized waves, i.e., $A_{DP} = A_H - A_V$, and is normally referred to as the specific differential attenuation. By analogy to equation (10) a linear relationship between A_{DP} and K_{DP} has been proposed (Bringi et. al., 1990) i.e.,

$$A_{DP} = b \cdot K_{DP} \quad (15)$$

Substituting equation (15) into (14) we get the following expression for the corrected Z_{DR}

$$Z_{DR}^{corrected}(r) = Z_{DR}^{measured}(r) + b\left[\Phi_{DP}(r) - \Phi_{DP}(0)\right] \quad (16).$$

The coefficient b is typically 0.01-0.003 at C-band (Bringi et. al., 2005).

5.3 Computation procedure

Similar to computing K_{DP}, correcting Z_{HH} and Z_{DR} for rain attenuation is rather challenging as the underlying $\Phi_{DP}(r)$ are very "noisy" i.e., generally contain many outliers. The current method used at DMI was inspired by Bringi et. al. (2005) and involve the following steps:

1. Compute the texture of Φ_{DP}, Tex($\Phi_{DP(x,y)}$), using equation (2).

2. Generate range mask based on thresholds for Tex($\Phi_{DP(x,y)threshold}$), Signal-to-Noise Ratio ($SNR_{threshold}$) and $r_{HVthreshold}$ to remove bad Φ_{DP} values.

3. Interpolate Φ_{DP} across "bad" data segments.

4. Compute the $\Phi_{DP}(0)$ i.e., offset at the "origin" by averaging the first N range gates Φ_{DP} containing precipitation.

5. $\Phi_{DP}(r)$ is then smoothed using a median filter with a window size of ~ 5.0 km - 6.5 km.

6. Correct both Z_{HH} and Z_{DR} for rain attenuation using equations (13) and (16), respectively.

6. Hydrometeor classifier

6.1 Introduction

Pixel based hydrometeor classification is carried out using the fuzzy logic methodology (Bringi and Chandrasekar, 2001, Zrnic et. al., 2001, Schuur et. al., 2003, Lim et. al., 2005). In the current approach, a given pixel of hydrometeor class j has a score S_j given by the relation

$$S_j = \frac{\sum_i w_i \cdot P_i}{\sum_i w_i} \qquad (17)$$

where P_i and W_i are the value of the parameter i, and the associated weight, for the class j. The radar parameters that have been used in the classifier are: Z_{HH}, Z_{DR}, K_{DP}, r_{HV}, plus the texture parameters, defined by equation (2), associated with Z_{HH}, Z_{DR}, Φ_{DP} (Schuur et. al., 2003, Sugier et. al., 2006). In fuzzy logic the values of the P_i for the different hydrometeor classes are described by the membership functions (MF) (see section 6.3).

6.2 Hydrometeor classes

In the current version of the algorithm the following 12 hydrometeor classes have been identified:

1. ground clutter,
2. sea clutter,
3. electrical signals from external emitters (EE) that interfere with our radars,
4. clean air echoes (CAE) such as from birds and insects,
5. drizzle,
6. light rain,
7. moderate rain,
8. heavy rain,
9. violent rain,
10. light snow,
11. moderate to heavy snow,
12. rain/hail mixture.

However, internally in the HMC software there are two classes each of ground and sea clutter, ten classes of external emitters including the signals from the sun and three classes of CAE. Further, the light rain class consists of four sub-classes; light drizzle, moderate drizzle, heavy drizzle and light rain.

6.3 Membership functions

In fuzzy logic the values of the P_i, in equation (17), for the different hydrometeor classes are described by the membership functions. In the current version the latter are expressed as Beta-functions of the type shown in fig. 8 with the 3 parameters: a, ß and g indicating the centre, half-

width at inflection point and the slope of the curve (Lim et. al., 2005).

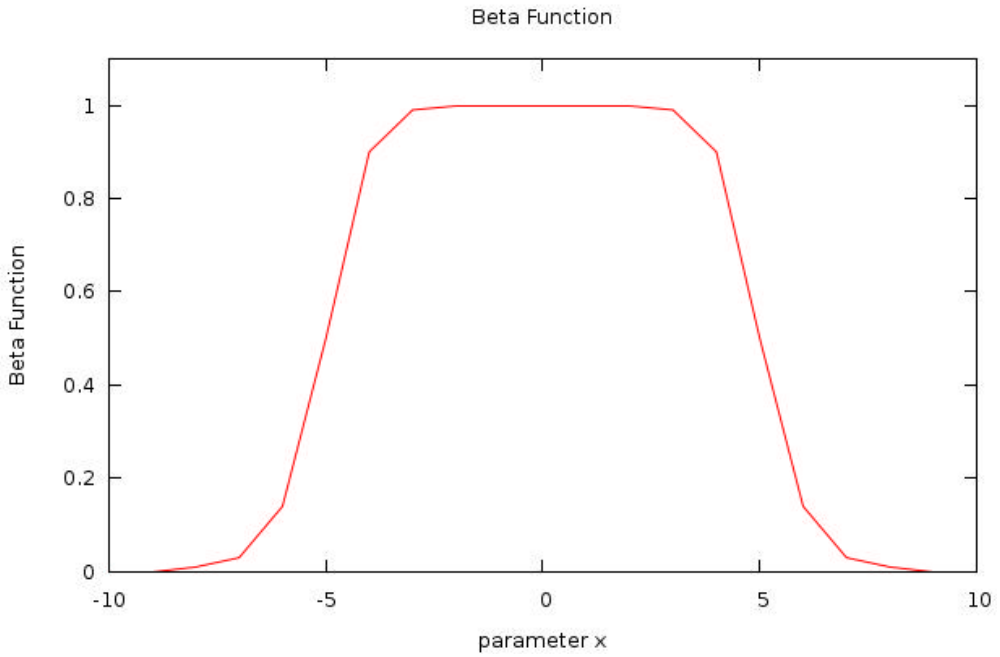

Fig. 8 Beta membership function

As a way of example, fig. 9 shows the membership functions for the parameter Z_{HH} for the different classes of rain.

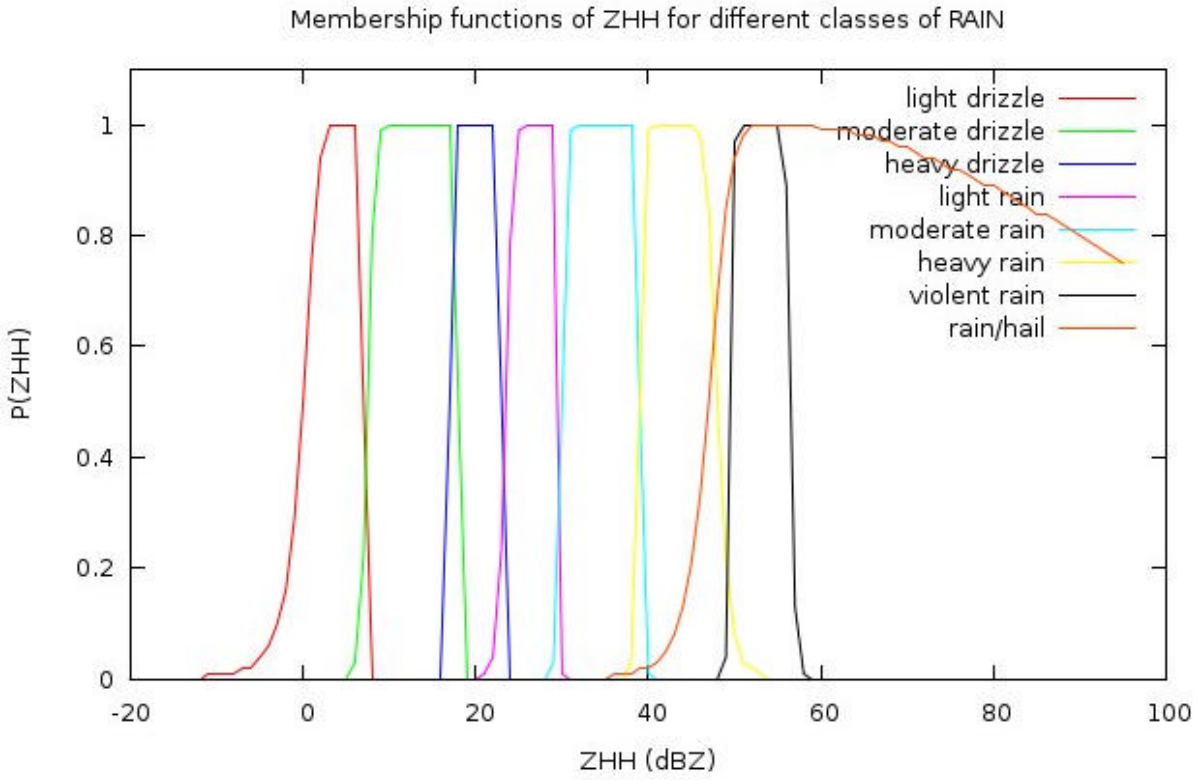

Fig. 9 Membership functions for Z_{HH} for different categories of rain.

Similar membership functions exits for other hydrometeor classes for Z_{HH} and for all the other

parameters used in the classification.

There has been much interest from international colleagues in the radar echo class 3 mentioned in section 6.2 above, because as far it is know, no hydrometeor classifier has included a class for the external emitters before (Gill et. al., 2012). For this reason the membership functions of Z_{HH}, Z_{DR} and r_{HV} for the different types of external emitters included in the classifier are given below (fig. 10). Also note radar echoes from the sun are also a sub-class of external emitters. Membership function of the sun plus those of external emitters for the parameter Z_{HH} can be seen in the bottom left part of fig. 10.

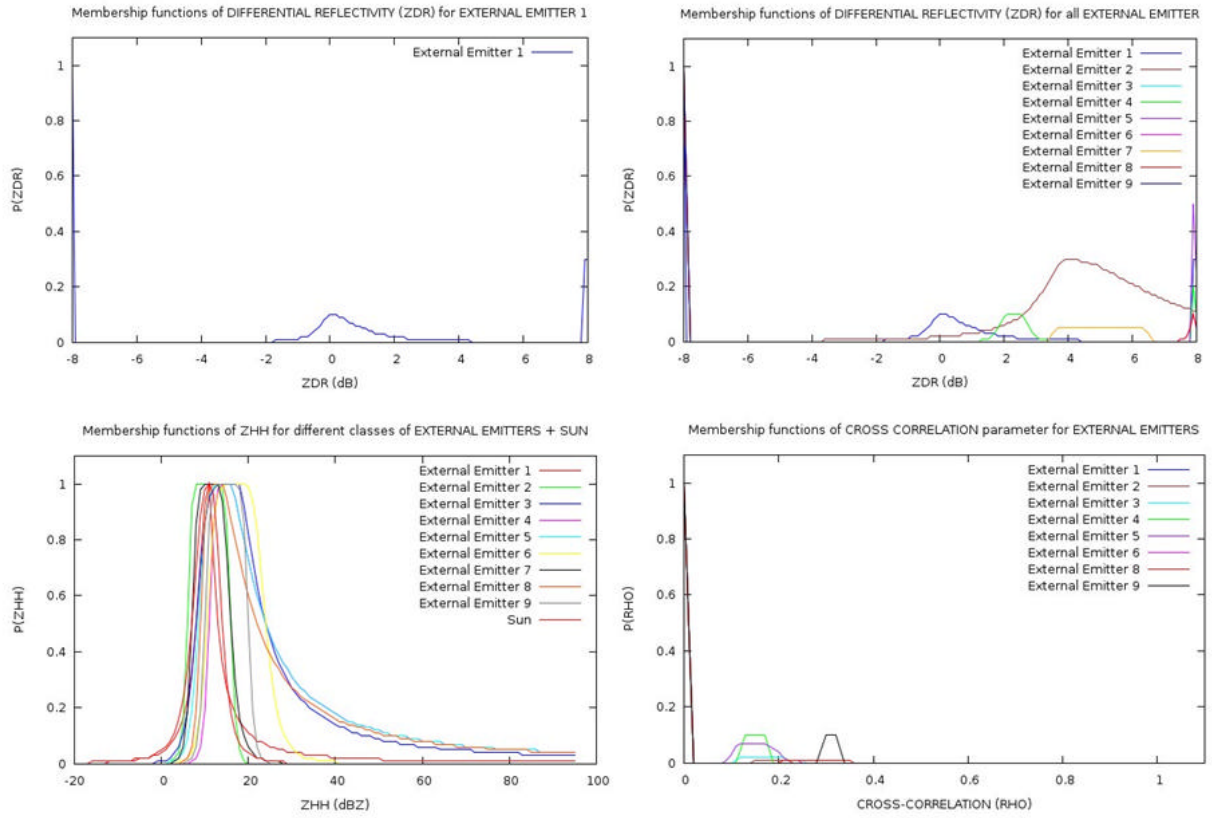

Fig. 10 Membership functions of Z_{HH}, Z_{DR} and r_{HV} for the different types of external emitters included in the classifier. Top left MF of a single external emitter of Z_{DR}. Top right MF of all 9 external emitters of Z_{DR}. Bottom left of all 9 external emitters and of sun of Z_{HH}. Bottom right MF of all 9 external emitters of r_{HV}.

6.4 Output from the hydrometeor classifier

The current version of the algorithm does the so-called level 1 and level 2 classifications. In the level 1 classification a radar echo is classified into one of four simple classes: precipitation, clutter, clean air echoes, and external emitters. Figure 11 shows an example of the output.

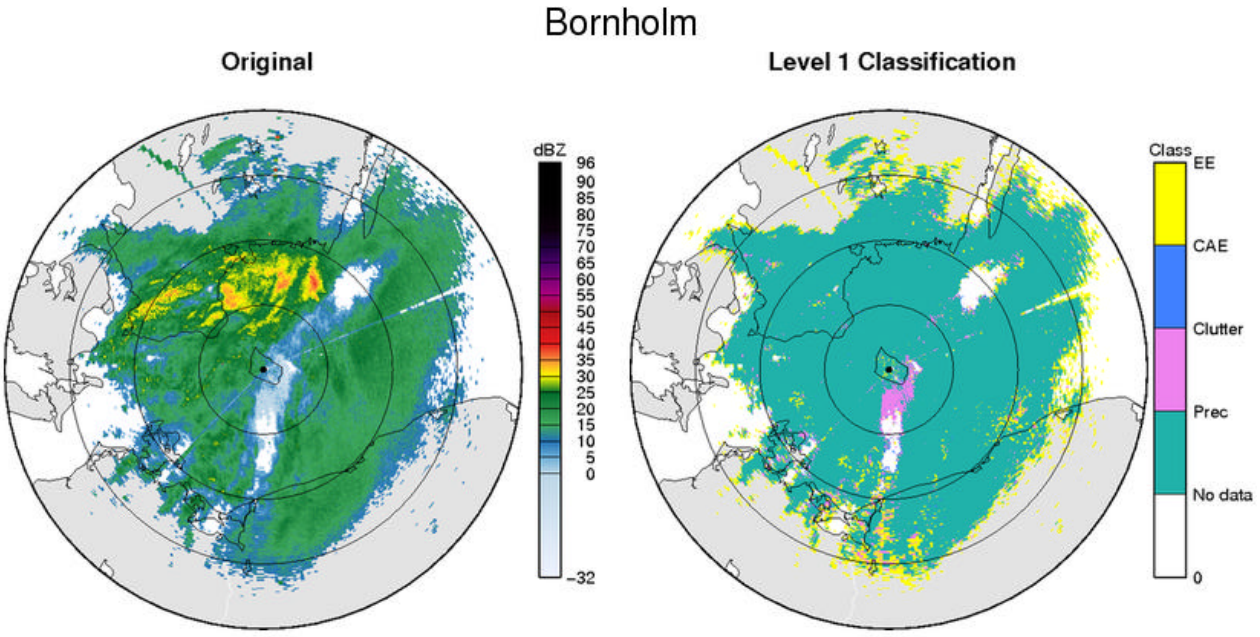

Fig. 11 shows radar image on the left (Z_{HH} original) and its corresponding level 1 hydrometeor classification into four classes: external emitters (EE), clean air echoes (CAE), clutter and precipitation (prec), colour code: yellow, blue, purple and green, respectively.

In the level 2 classification, the echoes that are classified as precipitation in level 1 are further sub-classified into different precipitation classes mentioned above. In this case the heights of the melting layer computed by the local NWP model and/or estimated from the radar parameters (see section 3) are used to strengthen the classification between the different classes of rain and snow. In the current version of the level-2 classification only the parameters Z_{HH}, $Z_{DR,}$ $K_{DP,}$ and r_{HV} are used. In particular, in this case score S_j is given by the relation

$$S_j = \frac{P^j{}_{Zhh} \cdot P^j{}_{height} \left[w_{Zdr} \cdot P_{Zdr}{}^j + w_{rhv} \cdot P^j{}_{rhv} + w_{Kdp} \cdot P^j{}_{Kdp} \right]}{w^j{}_{Zdr} + w^j{}_{rhv} + w^j{}_{Kdp}} \qquad (18)$$

Fig. 12 shows an example of the level 2 classification. Note that the radar data used to illustrate the classifications results are the same in figures 11 and 12.

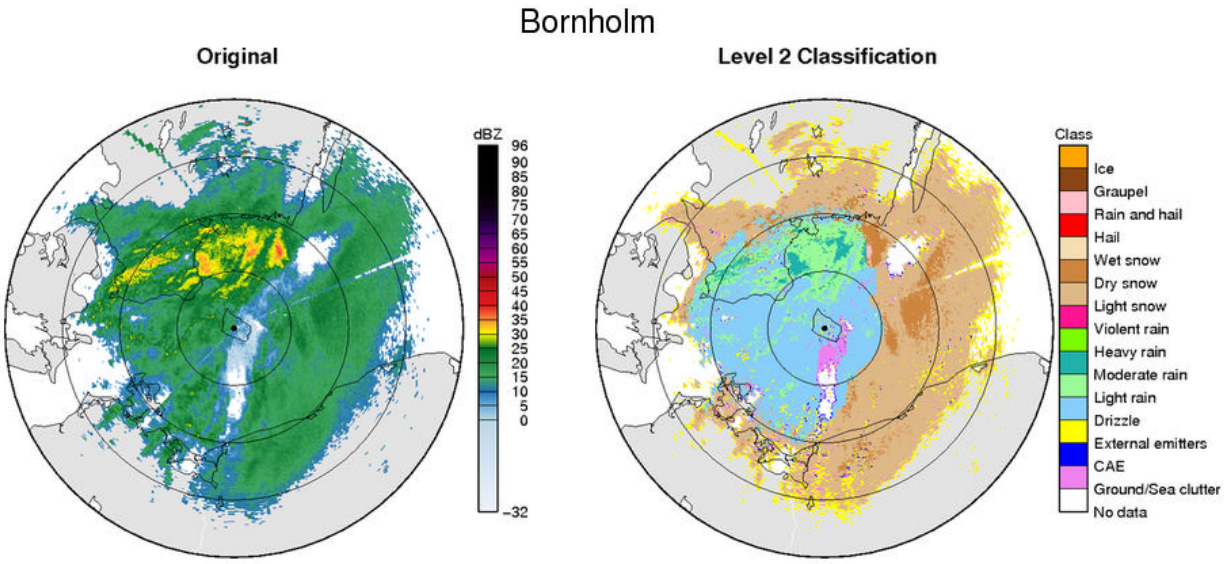

Fig. 12 shows radar image on the left (original Z_{HH}) and its corresponding level 2 hydrometeor classifications into eleven classes.

In addition to the above level 1 and 2 classifications, the algorithm can make use of the above classification output to remove the non-meteorological echoes in the original radar reflectivity product, Z_{HH}, shown on the left in each of the figures 11and 12. This is illustrated in figure 13 below. Concerning the latter product, it was the first product that was requested for routine operational use by the DMI end users, namely its meteorologists.

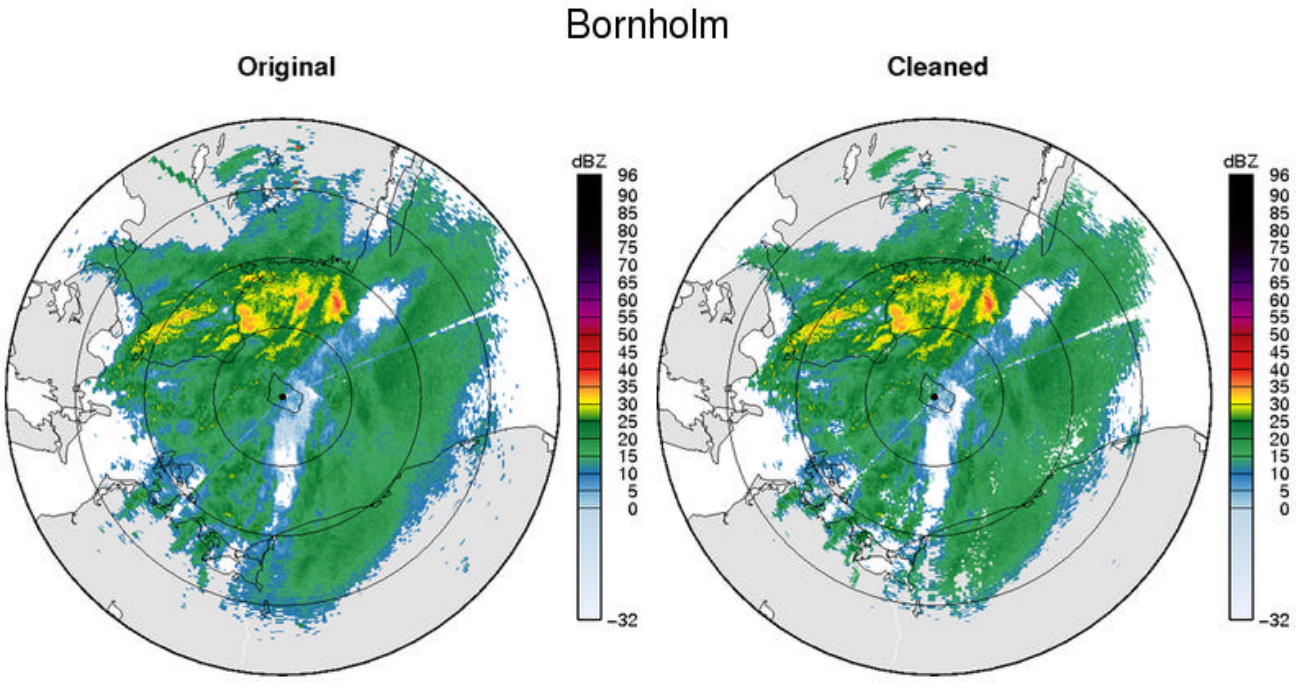

Fig. 13 shows the original radar product on the left and corresponding "cleaned" version on the right which has non-meteorological echoes removed.

6.5 Computational procedure

The software consists of two main modules:

A. Computation of all the radar parameters that are to be used in the fuzzy logic classifier
B. Using fuzzy logic rules classify each pixel of the radar returned echo into one of the predefined hydrometeor classes

The computational procedure involves the following steps for module A:

1. from the radar volume file read in the following radar parameters: reflectivity Z_{HH}, differential reflectivity Z_{DR}, cross correlation r_{HV}, differential phase Φ_{DP}, radial velocity V_r and spectral width W
2. by changing the default settings in the metadata file, choose whether to undertake the following operations:
    a. smooth Z_{DR} and r_{HV} parameters, by averaging over N number of range gates,
    b. correct Z_{DR} and r_{HV} at low signal-to-noise (SNR) ratio values,
    c. correct Z_{DR} and Φ_{DP} for radome effects,
    d. correct Z_{DR} and Φ_{DP} for potential biases,
    e. compute the specific differential phase, K_{DP}, as described in section 4 above,
    f. correct both Z_{HH} and Z_{DR} for rain attenuation as described in section 5 above,
3. now compute the following radar parameters in their appropriate units:
    a. Z_{HH} *(unit dBZ)* and its texture parameter, *Tex(*Z_{HH}*)*,
    b. Z_{DR} *(unit dB)* and its texture parameter, *Tex(*Z_{DR}*)*,
    c. r_{HV} and its texture parameter, *Tex(*r_{HV}*)*,
    d. Φ_{DP} *(unit deg.)* and its texture parameter, *Tex(*Φ_{DP}*)*,
    e. K_{DP} *(unit deg./km)* and its texture parameter, *Tex(*K_{DP}*)*,
    f. V_r *(unit m/s)* and its texture parameter, *Tex(*V_r*)*,
    g. W *(unit m/s)* and its texture parameter, *Tex(W)*,
    h. signal-to-noise ratio parameter, *SNR (unit dB)*, and
    i. the top, centre and bottom heights *(unit meters)* of the radar beam, *HTT*, *HTC* and *HTB*, respectively.

The computational procedure involves the following steps for module B:

1. read in all the computed radar parameters from module A
2. by changing the default settings in the metadata file, choose which of the above parameters are to be used for level-1 and level-2 hydrometeor classification
3. read-in a, ß and g indicating the centre, half-width at inflection point and the slope of the curve of the Beta functions (see fig. 8), for each radar parameter including the associated weights
4. for level-1 hydrometeor classification, for each radar echo
    a. get the "scores " of each of the parameter
    b. using fuzzy logic rules compute the final score for each predefined classes (precipitation, clutter, clean air echoes, and external emitters)
    c. classify the pixel by choosing the predefined hydrometeor class with the highest

score

5. for level-2 hydrometeor classification
    a. compute the heights of the melting layers using:
        i. the radar volume data, and
        ii. from Numerical Weather Prediction (NWP) models
    b. get the "scores " of each of the parameter
    c. using fuzzy logic rules compute the final score for each predefined classes (see section 6.2)
    d. classify the pixel by choosing the predefined hydrometeor class with the highest score

7. Summary

Hydrometeor classifier using the fuzzy logic method has been developed. The classifier make use of the dual polarization parameters Z_{HH}, Z_{DR}, K_{DP}, r_{HV}, plus the texture parameters associated with Z_{HH}, Z_{DR}, Φ_{DP} and the melting layer heights computed using the local NWP model forecasts. The latter are update every hour. In the current version of the algorithm, a radar echo can be classified into one of 12 classes. The subsequent versions of the algorithm will also include the following classes: hail, grapules, ice and rain/snow mixture.

Finally, the hydrometeor classifier described above has been developed with partial funding by the EU BALTRAD project which requires the software is made available according to open source principles (Michelson et. al, 2010). The software is thus available to the interested users. The Gnu Lesser general Public License policy shall apply.

Acknowledgements

The authors wish to thank Beatice Fradon for providing details of the data quality monitoring scheme at Meteo-France.

This work was partially financed by the EU (ERDF and ENPI) project BALTRAD, part of the Baltic Sea Region Programme 2007-2013.

References

Boumahmoud A-A., Fradon B., Roquain R., Perier L., and Tabary P., 2010, "The French operational dual-polarization processing chain", *ERAD 2010, 6th European conference on Radar in Meteorology and Hydrology.*

Bringi V. N., Chandrasekar N., Balakrishnan and Zrnic D. S., 1990, "An examination of propagation effects in rainfall on radar measurements at microwave frequencies", *J. Atmos. Oceanic Tech., vol., 7, 829 – 840.*

Bringi, V. N., Chandrasekar, V.: 2001, "Polarimetric Doppler Weather Radar", *Cambridge Univ. press, Cambridge, UK.*

Bringi V. N., Thurai R., and Hannesen R., 2005, "Dual-Polarization Weather Radar Handbook", *AMS-Gematronik GmbH.*

Carey L. D., Rutledge S. A., Ahijevych D. A., and Keenan T. D., 2000, " Correcting propagation effects in C-band polarimetric radar observations of tropical convection using differential propagation phase", *J. Appl. Meteor., vol. 39, 1405 – 1433.*

Doviak R. J. and Zrnic D.S., 1993, "Doppler radar and weather observations", 2nd edition, San Diego, CA. Academic Press.

Giangrande S. E., Krause J. M., and Kyzhkov, A.V., 2008,"Automatic designation of the Melting Layer with the Polarimetric Prototype of the WSR-88D Radar", *J. applied met. and climatology, vol. 47, 1354 – 1364.*

Gill R.S., Overgaard S. and Bøvith T. 2008,"Evaluation of the dual polarisation radar in an operational network", *ERAD 2008, 5th European conference on Radar in Meteorology and Hydrology, oral presentation.*

Gill R.S., Bøvith T., Sørensen M. B., Overgaard S. and Michelson D., 2010,"Development and evaluation of a BALTRAD dual polarisation hydrometeor classifier", *ERAD 2010, 6th European conference on Radar in Meteorology and Hydrology, oral presentation.*

Gill R.S., Sørensen M. B., Bøvith T., Koistinen J., Peura M., Michelson D., and Cremonini R., 2012,"BALTRAD dual polarization hydrometeor classifier", *ERAD 2012, 7th European conference on Radar in Meteorology and Hydrology.*

Lim S., Chandrasekar V., and Bringi V. N., 2005, "Hydrometeor classification system using dual-polarization radar measurements: Model improvements and in situ verification", *IEEE transactions of Geosciences and remote sensing, vol. 43, no. 4, 792-801.*

Michelson D., Szturc J., Gill R.S., Peura M, 2010, "Community-based weather radar networking with BALTRAD", *ERAD 2010, 6th European conference on Radar in Meteorology and Hydrology.*

Schuur, T., Ryzhkov A., and P. Heinselmann, 2003, "Observations and classification of echoes with the polarimetric WSR-88D radar, *NOAA National Severe Storms laboratory Tech. Report, Norman, Oklahoma, USA.*

Sugier, J., Tabary P., and J. Gourley, 2006, “Evaluation of dual polarization technology at C band for operational weather radar network, *report of the EUMETNET OPERA II, work packages 1.4 and 1.5.*

Tesud J., Le Bouar E., Obligis E., and Ali-Mehenni M., 2000, ”The rainfall profiling algorithm applied to polarimetric weather radar, *J. Atmos. Oceanic Technol., vol. 17, 322 – 356.*

Zrnic D. S., Ryzhkov A., Straka J., Liu Y., and Vivekanandan J., “Testing a procedure for automatic classification of hydrometeor types”, *J. atmospheric and oceanic technology, vol. 18, 892-913.*

Previous reports

Previous reports from the Danish Meteorological Institute can be found on:
http://www.dmi.dk/dmi/dmi-publikationer.htm